Robust DFT-based filtering of pulse-like FM signals corrupted by impulsive noise

Igor Djurović and Vladimir V. Lukin

Abstract— **Filtering of pulse-like FM signals with varying amplitude corrupted by impulse noise is considered. The robust DFT calculated for overlapped intervals is used for this aim. This technique is proposed in order to decrease amplitude distortion of output signals that can be introduced by the robust DFT calculated within a wide interval including possible zero-output. The proposed algorithm is realized through the following steps. In the first stage, the robust DFT is calculated for the intervals. Filtered signals from the intervals are obtained by applying the standard inverse DFT for the robust DFTs applied to input data. In the second stage, results for different overlapped intervals are combined using the appropriate order statistics. In addition, an algorithm inspired by the intersection of the confidence intervals rule is used for adaptive selection of the interval width in the robust DFT. Algorithm accuracy is tested on numerical examples. Computational complexity analysis is also provided.**

I. Introduction

Problem of filtering of pulse-like frequency modulated (FM) signals, corrupted by impulsive noise, is considered in this paper. These signals can be expressed by $x(n) = A(n)\exp(j\phi(n))$, where $A(n)$ and $\phi(n)$ are signal amplitude and phase, respectively. Particularly important classes of signals that could have such properties are: speech and old audio recordings [1], radar signals [2], and signals from computer networks [3], etc. Standard robust filters, such as the median filter and its variants [3]- [6], are lowpass and they can remove high frequency content from signals. The robust DFT filters proposed in [7] are designed for signals with a constant amplitude $A(n) = A$ and they can introduce distortion of amplitude in the case of signals with relatively fast variations of the signal amplitude.

Signal, Image and Video Processing, Vol. 1, No. 1, Mar. 2007

Two strategies for filtering FM signals corrupted by an impulse noise are proposed recently:

- filtering in time domain using the weighted myriad/median filters admitting negative weights [8]- [11];
- filtering in spectral domain using the robust DFT forms [12], [13].

Both groups are developed according to the fundamental concepts of robust statistics introduced by Huber [14], [15]. It has been shown in [7] that these two groups of techniques produce results of the same order of accuracy in signal filtering. The weighted median/myriad filters admitting negative weights require iterative or learning procedures for determination of weights that could be relatively complex. Also, these techniques require some kind of knowledge about a signal shape and characteristics of noise environment. However, application of the robust DFT is straightforward, since determination of the filter parameters does not require a complicated procedure.

For pulse-like FM signals, the robust DFT applied to entire observation, as it is done conventionally [7], could treat some signal samples as outliers and produce distorted amplitude or even zero-output. Here we propose segmentation of a signal into overlapped or non-overlapped intervals (segments) and application of the robust DFT filtering technique on intervals. In the case of non-overlapped intervals, output of the resulting filter is equal to outputs of filters calculated for the corresponding intervals. Since the main problem in the case of shorter intervals could be residual noise, we propose that in the case of overlapped intervals the output of the filter can be obtained on the basis of order statistics (median or L-filter form) [16].

A particular by interesting issue is adaptive determination of interval length in the robust

DFT for the considered class of signals. Our goal is to design a robust filter in such a manner that for an interval where there is no signal, or signal has a constant or almost constant amplitude, the interval is selected as wide as possible in order to reduce the noise influence. However, for rapidly varying signal amplitude region we would like to select a relatively small interval in order to preserve signal amplitude and other details. In this technique we filter signals with the robust DFT applied to non-overlapped intervals (extension to the overlapped intervals is straightforward). The intersection of the confidence interval (ICI) rule, recently proposed by Katkovnik and his co-workers, is used here for this application [17]-[19]. The ICI algorithm produces a trade-off between noise influence and distortion of signal amplitude.

The paper is organized as follows. Review of the robust DFT is given in Section II with a highlighted problem that appears in the case of signals with relatively short duration. The proposed technique for filtering based on the robust DFT applied on intervals is presented in Section III. Computational complexity study with a brief analysis of the achieved accuracy is also given in this section. Examples and simulation results with both overlapped and non-overlapped intervals are given in Section IV. An adaptive algorithm that selects interval width according to the ICI rule is proposed in Section V, with examples demonstrating its accuracy.

II. Robust DFT - An overview

A. Common robust DFT forms

The standard DFT is defined as:

$$X(k) = \frac{1}{N}\sum_{n=0}^{N-1} x(n)W_N^{kn}$$
$$= \text{mean}\{x(n)W_N^{kn}|n \in [0, N)\} \qquad (1)$$

where $W_N = \exp(-j2\pi/N)$. This and other linear techniques are sensitive to the impulse noise influence [4]. In order to handle an influence of impulse noise, several robust DFT forms have been proposed [12], [20] - [22]. Here, we will consider the marginal-median DFT presented in [21]. It belongs to a wider class of the L-DFT forms defined as [22]:

$$X_\alpha(k) = \sum_{i=0}^{N-1} a_i[\mathbf{r}_k(i) + j\mathbf{i}_k(i)], \qquad (2)$$

$$\mathbf{r}_k(i) \le \mathbf{r}_k(i+1) \qquad \mathbf{i}_k(i) \le \mathbf{i}_k(i+1)$$

where $\mathbf{r}_k(i)$ and $\mathbf{i}_k(i)$ are sorted elements from the sets:

$$\mathbf{r}_k(i) \in \{\text{Re}\{x(n)W_N^{kn}|\}|n \in [0, N)\}$$
$$\mathbf{i}_k(i) \in \{\text{Im}\{x(n)W_N^{kn}|\}|n \in [0, N)\}. \qquad (3)$$

The weighting coefficients can be selected as:

$$a_i = \begin{cases} 1/N(1-2a) & i \in [aN, N-aN) \\ 0 & \text{elsewhere} \end{cases} \qquad (4)$$

where $a \in [0, 0.5]$. The L-DFT with coefficients (4) is commonly referred to as the $\alpha-$trimmed DFT. For $a = 0$ the standard DFT follows, with exact spectral estimation for noiseless signal and ML estimate for signals corrupted by Gaussian noise. The marginal-median DFT form follows for $a = 0.5 - 1/N$. It is robust to the impulse noise influence but it is calculated by using just two modulated signal samples causing the spectral distortion effect. Then we can expect that there is the L-DFT (or $\alpha-$trimmed mean DFT) form that produces a trade-off between the noise influence and spectral distortion effects. Several procedures for designing adaptive L-DFT (and adaptive myriad DFT) forms are proposed in [22], [23]. Since design of the optimal L-DFT is not the main goal of this paper, we will consider the marginal-median DFT form but we note that the procedures similar to the ones from these papers could be applied to any adaptive or non-adaptive robust DFT forms (both L-filter and myriad). Signal denoising based on the robust DFT can be performed as [7]:

$$\hat{f}(n) = \sum_{k=0}^{N-1} X_\alpha(k)W_N^{-kn}. \qquad (5)$$

B. Drawback of the L-DFT forms

In order to describe the drawback of the considered robust techniques (in particular L-

DFT forms) we consider the following signal:

$$x(n) = \begin{cases} e^{(j\omega_0 n)} & n \in [\frac{N}{2} - \frac{K}{2}, \frac{N}{2} + \frac{K}{2}] \\ 0 & \text{elsewhere} \end{cases} \quad (6)$$

where $K < N/2$ and N is the number of samples used to evaluate of the DFT. A set of real values of the modulated signal samples $\{\text{Re}\{x(n)W_N^{kn}|\}|n \in [0, N)\}$ (similar situation holds for imaginary parts) has at most $(2K+1) < N$ nonzero samples. The remaining $N - (2K+1)$ samples would be equal to zero and these samples are positioned between positive and negative elements in the sorted sequence with significant probability that the median and other close samples in the sorted sequence (which is assumed to be noise-free) be equal or close to zero and producing zero-output almost everywhere, i.e., output with distorted amplitude. A situation becomes even worse in the case of signals with a smaller number of non-zero samples. Then, instead of significant benefit (removing impulse noise), we get a zero output, i.e., filter performs absolutely incorrectly. This kind of problem is very important since some of the most important potential applications of the robust DFTs are filtering of old audio records [1] and radar signal processing [2], where signal components that may have abrupt appearance and/or disappearance can take place.

Example. In order to demonstrate described filtering problem we considered two signals:

$$f_i(t) = \exp(j32\pi t - b_i t^2), \quad (7)$$

where $i = 1, 2$ and $b_1 = 6$ and $b_2 = 24$. Our signal is considered within $t \in [-1, 1)$ and sampled with the rate of $\Delta t = 1/512$ (1024 samples in total). Output of the robust DFT-based filters for noiseless signals is given in Figs. 1 and 2. For the first signal with $b_1 = 6$, it can be seen that the marginal-median form produces distorted signal amplitude. By decreasing a we are achieving a gradual improvement in representing signal amplitude. However, results that have distorted samples around the maximum of magnitude, $t = 0$, are obtained even for $a = 1/8$. Situation is worsened in the case of a signal with narrower component having high amplitude ($b_1 = 24$), where all L-DFT forms produce significantly distorted outputs (see Fig. 2). It is worth to note that the decrease of a increases the noise influence and that the reducing of a would not improve results for noise environment. Therefore, reducing a in order to remove spectral distortion effect is not a reasonable solution for signals corrupted by an impulse noise. A technique for handling this issue based on the segmentation of the signal in non-overlapped or overlapped regions will be described in the next section.

III. Proposed filtering technique

A. Intervals

In order to overcome problems arising in the case of signals with fast variations in the signal amplitude, consider a signal $x(n)$ segmented into intervals. Non-overlapped intervals can be written as:

$$x_i(n) = x(n + iN/Q), \quad (8)$$
$$i \in [0, Q),\ n \in [0, N/Q)$$

where Q is a number of intervals, and N/Q is assumed to be an integer. Alternatively, overlapped intervals can be written as:

$$x_i(n) = x(n + i\delta N/Q), \quad (9)$$
$$i \in [0, Q/\delta),\ n \in [0, N/Q)$$

where $\delta \in (0, 1]$ is a measure of intervals' overlap. For $\delta = 1$ intervals are non-overlapping, while with $\delta < 1$ the intervals overlap. Overlapping intervals with two different values of δ are shown in Fig. 3. Note that dividing signals into intervals and obtaining spectral estimation from these intervals is a common technique in spectral analysis [24], [25], DCT based denoising [26], etc.

Our idea is to perform filtering in narrow intervals by the robust DFT. For narrow intervals it can be expected that the amplitude distortion will be small since, as predicted, within such intervals the observed variations in the amplitude are smaller than in the wider interval.

The proposed algorithm can be described as follows.

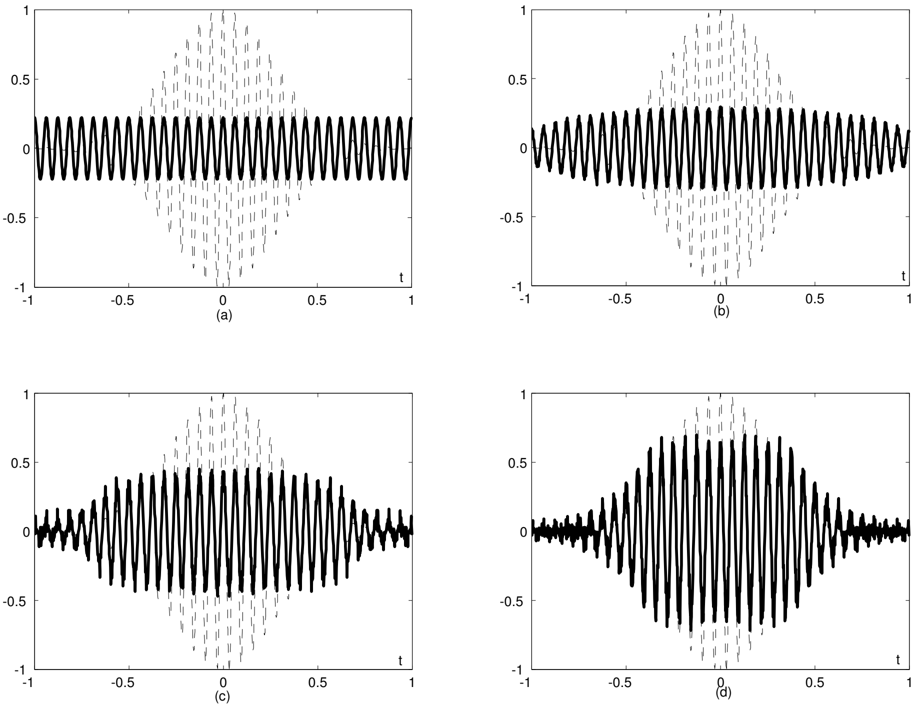

Fig. 1. Denoising of the signal $\exp(j32\pi t)\exp(-6t^2)$ by using: (a) marginal-median DFT; (b) α-trimmed mean DFT with $a = 3/8$; (c) α-trimmed mean DFT with $a = 1/4$; (d) α-trimmed mean DFT with $a = 1/8$. Dashed line - original signal; Solid line - filtered signal.

Step 1. Segmentation into intervals (8) or (9).

Step 2. Calculation of the robust DFT for intervals (any robust DFT form could be used; here the marginal-median DFT will be applied) $X_i(k)$, $i \in [0, Q/\delta)$.

Step 3. Calculation of the signal estimation (filtered signal) for intervals by using the standard inverse DFT:

$$f_i(n) = IDFT\{X_i(k)\}. \tag{10}$$

Step 4. For non-overlapped intervals output of the proposed filter can be calculated as:

$$\hat{f}(n+iN/Q) = f_i(n) \quad i \in [0, Q),\ n \in [0, N/Q), \tag{11}$$

while for the overlapped intervals filtered signals $f_i(n)$ should be combined in some appropriate manner.

B. Combining the results from subintervals

We can establish the following relation between filtered signals from intervals $f_i(n)$ and filtered signal $\hat{f}(n)$ for entire interval

$$\hat{f}(n + i\delta N/Q) = f_i(n), \tag{12}$$

$$i \in [0, Q/\delta),\ n \in [0, N/Q).$$

However, for $\delta < 1$ we can obtain several estimates produced by various intervals for a single instant. There are numerous schemes that can be employed for this purpose. Since in our application the main problem could be the remaining residual impulse noise, we decided to apply the median estimate to produce the output signal for a given instant. This can be done for $\delta < 1/2$ when we have more than two estimates for each instant.

Three characteristic cases are depicted in Fig. 3. In the first case (Fig. 3a) we have $Q = 4$ non-overlapped intervals. In the second one (Fig. 3b) we have $Q = 4$ and interval overlapping with $\delta = 1/2$, i.e., for each instant we have two estimates produced by two different intervals (for one particular instant these

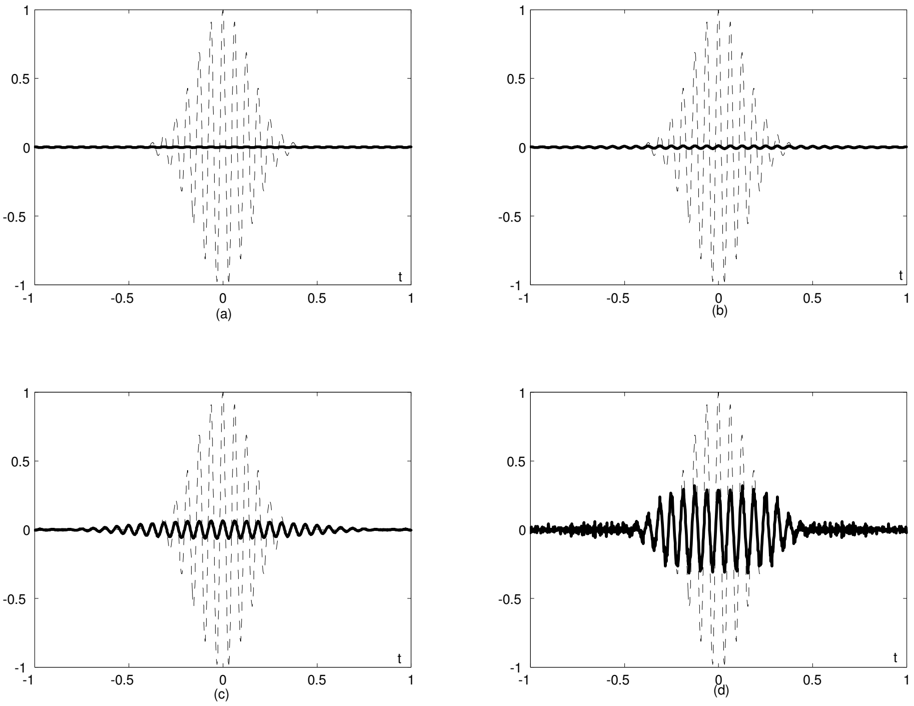

Fig. 2. Denoising of the signal $\exp(j32\pi t)\exp(-24t^2)$ by using: (a) marginal-median DFT; (b) α-trimmed mean DFT with $a = 3/8$; (c) α-trimmed mean DFT with $a = 1/4$; (d) α-trimmed mean DFT with $a = 1/8$. Dashed line - original signal; Solid line - filtered signal.

estimates are depicted with small circles). Finally, in Fig. 3c, one can see overlapping with $\delta = 1/8$ where for each instant we can have up to 8 different estimates produced with different intervals (again marked with small circles for the considered instant).

C. Computational complexity

The proposed technique that improves filtering of FM signals with short components embedded in an impulse noise decreases computational complexity with respect to the robust DFT calculated over entire interval. We can have Q non-overlapped or Q/δ overlapped intervals of the width N/Q.

The following main operations are performed within the algorithm:

- N/δ complex multiplications $x(n)W_N^{kn}$;
- $2\frac{N^2}{\delta Q}\log_2 N - 2\frac{N^2}{\delta Q}\log_2 Q$ comparisons for sorting of real and imaginary parts of modulated signal sequences;
- N/δ real multiplications of sorted elements from sequences with a_i (4);
- $\frac{N}{\delta}\log_2 N - \frac{N}{\delta}\log_2 Q$ complex multiplications and complex additions for implementation of the inverse FFT, (5);
- $2(N/\delta)\log_2(1/\delta)$ comparisons for median filtering in the case of the overlapped intervals.

Note that it is assumed that some fast sorting procedure, such as the quicksort, is employed and that it can, under some conditions, require $(N/Q)\log_2(N/Q)$ comparisons for sorting a sequence of (N/Q) samples. It can be seen that sorting of real and imaginary parts of modulated signal sequences is a dominant operation in the algorithm (function of $(N^2/\delta Q)\log_2 N$) and we can conclude that number of operations is decreased approximately $Q\delta$ times with respect to the evaluation in the case of the robust DFT evaluated over the entire interval ($Q = 1$ and $\delta = 1$).

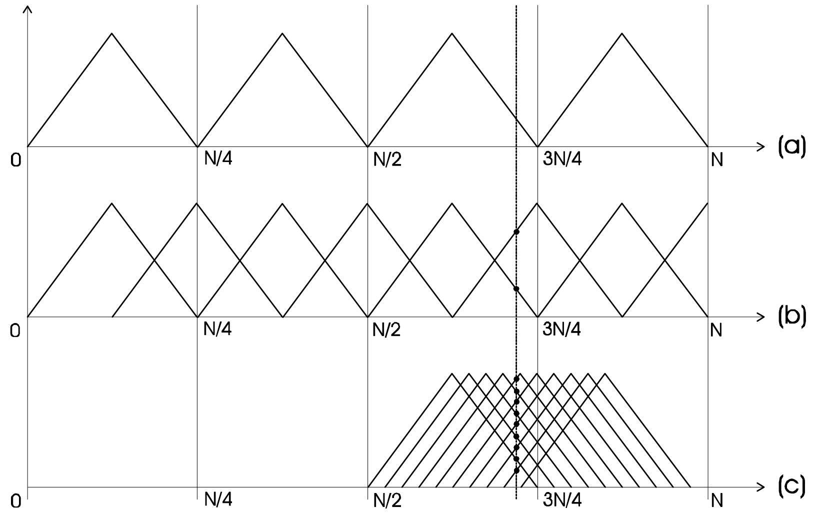

Fig. 3. Illustration of segmentation of signals into subintervals: (a) Nonoverlapped intervals $Q = 4$; (b) Overlapped intervals with $\delta = 1/2$ - up to 2 estimates for instant; (c) Overlapped intervals with $\delta = 1/8$ - up to 8 estimates for each instant.

D. Noise influence

As was already mentioned, one drawback of the proposed technique with reducing interval width is increasing the estimator variance. Namely, it has been shown that variance of the robust DFT is approximately [13]:

$$\sigma^2 \approx \frac{1}{N} \frac{\int_{-\infty}^{\infty} (F'(\zeta))^2 p_\nu(\zeta) d\zeta}{\left[\int_{-\infty}^{\infty} F''(\zeta) p_\nu(\zeta) d\zeta\right]^2} \tag{13}$$

where $p_\nu(\zeta)$ is the probability density function (pdf) of the considered additive noise. Function $F(\zeta)$ is commonly referred to as the loss-function ($F'(\zeta)$ and $F''(\zeta)$ are its first and second derivatives) and it determines the used DFT form. For example, $F(\zeta) = |\zeta|^2$ corresponds to the standard DFT while $F(\zeta) = |\zeta|$ determines the median DFT form. For details we refer readers to [13]. The resulting variance of the marginal-median DFT is:

$$\sigma^2 \approx \frac{1}{N} \frac{1}{4p_\nu^2(0)}. \tag{14}$$

It can be seen that the variance increases with a decrease of the interval width. Then, it can be expected that there is a trade-off between distortion effects introduced by a wide interval and noise influence (more emphatic for narrow intervals). A technique for achieving this trade-off (or results close to the trade-off) will be studied in Section V.

IV. Simulation study

We perform calculation study for three signals:

$$f_{1,i}(t) = e^{(j32\pi t)} e^{(-\beta_i (t-t_0)^2)},$$

$$f_{2,i}(t) = e^{(j212\pi t)} e^{(-\beta_i (t-t_1)^2)},$$

$$\begin{aligned} f_3(t) \;\; &= \;\; e^{(j32\pi t)} e^{(-32(t-t_0)^2)} \\ &\quad + e^{(j212\pi t)} e^{(-128(t-t_1)^2)}. \end{aligned} \tag{15}$$

where $f_{1,i}(t)$ and $f_{2,i}(t)$ are low frequency signal and high frequency signal, respectively, while $f_2(t)$ is sum of two signals.

For the signals $f_{1,i}(t)$ and $f_{2,i}(t)$ we performed tests with various values $\beta_i = 3 \cdot 2^i$ for $i = 1, 2, ..., 6$. These values of β_i correspond to relatively wide (small β_i) and relatively narrow (large β_i) pulse-like signals. In total, we have 13 signals in our study. In all experiments, signals have been considered within $t \in [-1, 1)$, sampled with $\Delta t = 1/512$ (the number of samples was $N = 1024$). Instants

t_0 and t_1 in the Monte Carlo simulation are selected randomly according to an uniform probability law within the interval $[-1, 1]$.

Signals are embedded in the symmetric $\alpha-$stable noise environment. This class of noises is assumed to accurately model numerous practically observed noise environments. Detailed analysis of this noise can be found in [27], [28]. It has two parameters (α, γ), where $\alpha \in [0, 2]$ and it controls impulsiveness of the noise, while γ is the dispersion factor that corresponds to the noise strength. Impulsiveness of the noise increases with a decrease of α. Two particular members of the $\alpha-$stable class are the Gaussian noise with $\alpha = 2$ (variance of this noise is 2γ) and the Cauchy noise with $\alpha = 1$. We have performed an analysis for $\alpha = 0.1i$ where $i = 1, 2, ..., 20$ and for $\gamma = 10^{-l/10}$ for $l = 0, 1, ..., 20$. However, due to the brevity reasons, the results obtained only with $\gamma = 0.1$ and $\alpha = 1$ (Cauchy noise) will be demonstrated here for some of the signals from (15).

First, we demonstrate results of the applied algorithm with various parameters for the test signal $f_{1,6}(t)$ (narrow signal with $\beta_6 = 192$) (see Fig. 4), and for the test signal $f_{2,3}(t)$ (relatively wide signal with $\beta_3 = 24$), Fig. 5. Both signals are centered around $t_0 = t_1 = 0$. Fig. 4a represents the useful signal (thick line) and the signal corrupted by noise (dashed line). In all other subplots in Fig. 4, the original signal is represented with dashed line, while the filtered signals are given with thick lines. The parameters of the algorithm are given in the top right corner of subplots where 'ov' denotes overlapped intervals with $\delta = 2/Q$ and 'no' denotes non-overlapped intervals. It may be observed that the wider non-overlapped intervals introduce a significant distortion of the signal amplitude. However, narrower intervals have emphatic noise influence with accurate tracking of the signal amplitude. From all illustrations, an improvement that can be achieved by overlapped intervals is obvious.

The second demonstration is with the wider signal ($\beta_3 = 24$) of higher frequency. Here, we give only noiseless signal in Fig. 5a, while in other subplots the filtered signals are given. Since this signal is wider, relatively small amount of the spectral distortion is achieved even with the relatively wide interval of $N/Q = 64$. Other conclusions that can be drawn from this illustration are similar to the case of the signal $f_{1,6}(t)$ (Fig. 4). Both illustrations (Figs. 4 and 5) confirm that it would be very desirable to have an algorithm that could select the wide window in the region of signal without variations in the amplitude (both without signal and with almost constant amplitude) and a rather narrow interval for the region of varying amplitude.

Tables I-VII represent results of the Monte Carlo simulations for $R = 1000$ trials for the signals: $f_{1,1}(t)$, $f_{1,3}(t)$, $f_{1,6}(t)$, $f_{2,1}(t)$, $f_{2,3}(t)$, $f_{2,6}(t)$, and $f_3(t)$, respectively. The considered noise was Cauchy noise ($\alpha = 1$) with $\gamma = 0.1$. Signals are filtered with various parameters of the filters. The accuracy is measured in terms of the mean absolute error (MAE) and the root mean squared error ($RMSE$):

$$MAE = \frac{1}{R}\frac{1}{N}\sum_{r=1}^{R}\sum_{n=1}^{N}|\hat{f}_r(n) - f(n)| \quad (16)$$

$$RMSE = \sqrt{\frac{1}{R}\frac{1}{N}\sum_{r=1}^{R}\sum_{n=1}^{N}[\hat{f}_r(n) - f(n)]^2}, \quad (17)$$

where $f(n)$ is the original non-noisy signal, while $\hat{f}_r(n)$ is the output of the corresponding filter in the r-th trial.

In addition, since the main interest is in quality of filtering in the region with the signal with significant magnitude, we have considered the following local measures given by eq. (18) and eq. (19) at the top of the next page, where N_l is the number of samples in which the signal amplitude is relatively large, i.e., above some specific threshold. We adopted that such samples are selected as $|f(n)| > \varepsilon \max |f(n)|$, where $\max |f(n)|$ is the maximal value of signal magnitude and ε is a threshold in our research set to $\varepsilon = 0.1$.

Results in Table I-VII are given in terms of the number of intervals Q. The best results are highlighted. It can be seen that, in almost all experiments presented in these tables, the best results are achieved with $Q = 16$ ($N/Q = 64$) and overlapped intervals when the

$$MAE_l = \frac{1}{R}\frac{1}{N_l}\sum_{r=1}^{R}\sum_{n=1,|f(n)|>\varepsilon \max|f(n)|}^{N} |\hat{f}_r(n) - f(n)| \tag{18}$$

$$RMSE_l = \sqrt{\frac{1}{R}\frac{1}{N_l}\sum_{r=1}^{R}\sum_{n=1,|f(n)|>\varepsilon \max|f(n)|}^{N} [\hat{f}_r(n) - f(n)]^2}, \tag{19}$$

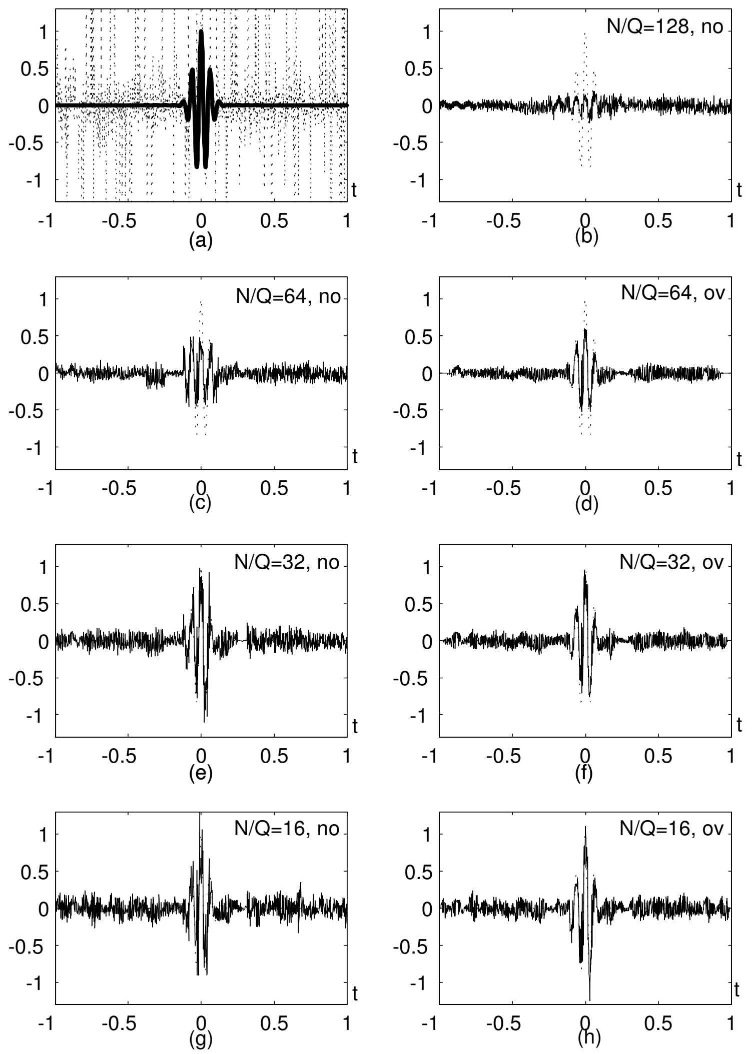

Fig. 4. Filtering of the signal $f_{1,6}(t)$ embedded in the α-stable noise with $\gamma = 0.1$ and $\alpha = 1$: (a) Noisy signal - dashed line; original signal - thick line; (b) The signal filtered with $N/Q = 128$ with non-overlapped intervals; (c) The signal filtered with $N/Q = 64$ with non-overlapped intervals; (d) The signal filtered with $N/Q = 64$ with overlapped intervals; (e) The signal filtered with $N/Q = 32$ with non-overlapped intervals; (f) The signal filtered with $N/Q = 32$ with overlapped intervals; (g) The signal filtered with $N/Q = 16$ with non-overlapped intervals; (h) The signal filtered with $N/Q = 16$ with overlapped intervals. In subplots (b)-(h) thin dotted lines represent original non-noisy signal.

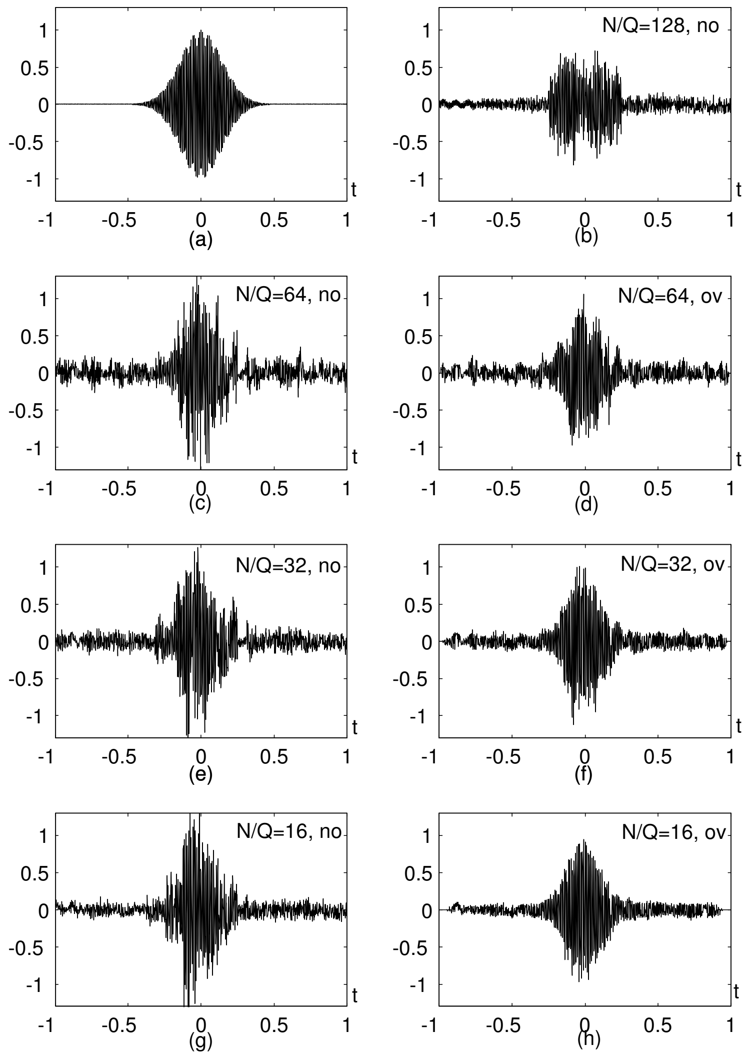

Fig. 5. Filtering of signal $f_{2,3}(t)$ embedded in the α-stable noise with $\gamma = 0.1$ and $\alpha = 1$: (a) The original signal - thick line; (b) The signal filtered with $N/Q = 128$ with non-overlapped intervals; (c) The signal filtered with $N/Q = 64$ with non-overlapped intervals; (d) The signal filtered with $N/Q = 64$ with overlapped intervals; (e) The signal filtered with $N/Q = 32$ with non-overlapped intervals; (f) The signal filtered with $N/Q = 32$ with overlapped intervals; (g) The signal filtered with $N/Q = 16$ with non-overlapped intervals; (h) The signal filtered with $N/Q = 16$ with overlapped intervals.

signal is considered in entire intervals. The reason is the fact that the measures (MAE and $RMSE$) take both samples belonging to signal and to noise-only region with the same weight and, on average, the best results are obtained by this filter. As one can see from Figs. 4 and 5, this is true for noise only region but it is not absolutely true for the signal region. Then, better results for this region can be achieved for narrower intervals (larger number of intervals). From the tables one can notice a significant improvement achieved when overlapped intervals are used. Also, it can be seen that for some signals the best results in terms of the $RMSE$ are achieved with $Q = 1$ (very short signals $f_{1,6}(t)$ and $f_{2,6}(t)$), i.e., for evaluation of the algorithm in the entire interval. It is the case for very narrow signal, where noise-only region gives the biggest contribution to the accuracy measure. However, in numerous applications we are more interested in filtered output in signal regions rather than in the noise only regions. Then this kind of accuracy measure could lead to a wrong conclusion. It is the reason to consider alternative measures (18) and (19), where the criteria are evaluated just for intervals of significant signal magnitude. Here, we can see that for the signals $f_{1,1}(t)$, $f_{1,3}(t)$, $f_{2,1}(t)$, $f_{2,3}(t)$, and $f_3(t)$, the best results are achieved with $Q = 16$ (the width of the interval is 64 samples), see Tables I, II, IV, V and VII. However, for the signals $f_{1,6}(t)$ and $f_{2,6}(t)$ with a short non-zero interval, the best results are achieved for the narrower intervals $N/Q = 32$, i.e., $Q = 32$.

V. Adaptive segmentation

From the previous analysis it is obvious that a desired filtering technique would be able to select wide intervals for noise only regions and regions with a constant signal amplitude, and to select narrower intervals for regions with fast variations in the signal amplitude. At the same time, we should take care of the noise influence that is more emphatic for narrower intervals. One of potential solutions for similar problems with a trade-off between accuracy of technique for regions with variations in the model and noise influence, are the intersection of the confidence intervals (ICI) rule algorithms. These algorithms were initially proposed in [29], and further developed and applied to numerous signal processing problems [18], [30].

Here we give a brief description of the ICI algorithm and later we describe the technique for its application to the considered problem. The algorithm considers estimates achieved with various parameters ξ_i from the set Ξ. These estimates are denoted as $p(n;\xi_i)$, where n is a considered time instant. Parameters ξ_i are sorted in such a manner that the influence of inaccuracy of the model is the smallest for ξ_1 and larger for any subsequent parameter from the set Ξ. Let a standard deviation of the estimator with parameter ξ_i be denoted as $\sigma(n;\xi_i)$. Then, the ICI algorithm in the basic form can be summarized as:

Step 1. Set that an initial estimate is obtained with parameter ξ_1 that introduces the smallest inaccuracy for abrupt changes in the signal model $p_e(n) = p(n;\xi_1)$. Set $i = 1$.

Step 2. If the condition:

$$|p(n,\xi_{i+1}) - p(n;\xi_i)| \le \kappa[\sigma(n;\xi_{i+1}) + \sigma(n;\xi_i)], \tag{20}$$

is satisfied, set $i = i + 1$ and repeat this step; otherwise proceed to step 3.

Step 3. Take that an estimate for a given n is $p_e(n) = p(n;\xi_i)$ with the adaptive parameter given as $\xi_e(n) = \xi_i(n)$.

This procedure is very fast since it includes only comparisons. However, it requires that we have estimates obtained with different parameters ξ_i. Parameter κ determines a width of the confidence interval and its appropriate selection is crucial for the algorithm accuracy [30].

For filtering of FM signals with varying amplitude corrupted by impulse noise, we will apply this algorithm in the following form. The set of segments widths $\Xi = \{\xi_i, i = 1, ..., \Pi\}$ is considered, with $\xi_i = (N/Q_i)$. The width of intervals is increasing, $\xi_i < \xi_{i+1}$, since narrower intervals produce smaller errors for signals with fast amplitude variations. The main problem in our algorithm is the fact that we do not know $\sigma(n;\xi_i)$ since the parameters of the noise are unknown. However, we know that the output variance of our filter is inversely proportional to the width of the interval $\sigma^2(n;\xi_i) \equiv \rho^2/\xi_i$, (13). The constant ρ^2 is unknown for unknown pdf of noise. Then, condition (20) can be written as:

$$|\hat{f}_{\xi_{i+1}}(n) - \hat{f}_{\xi_i}(n)| \le \kappa\rho \left[\frac{1}{\sqrt{\xi_{i+1}}} + \frac{1}{\sqrt{\xi_i}}\right]. \tag{21}$$

where $\hat{f}_{\xi_i}(n)$ is the signal filtered with segments of the width ξ_i, while ρ represents a multiplicative constant for the standard deviation of the estimator $\sigma(n;\xi_i) = \rho/\sqrt{\xi_i}$. The remaining problem is a determination or estimation of ρ. However, here we have two unknown constants, ρ and κ. We propose to apply the cross-validation (CV) algorithm for determi-

TABLE I

Integral and local MAE and RMSE in filtering of $f_{1,1}(t)$ corrupted with Cauchy noise with $\gamma = 0.1$. Index l in this and subsequent tables denotes statistics evaluated locally in the region of signal with relatively high amplitude.

	$Q = 1$,no	$Q = 2$,no	$Q = 4$,no	$Q = 8$,no	$Q = 16$,no
RMSE	0.3744	0.3844	0.3399	0.3393	0.3500
MAE	0.2931	0.3031	0.2578	0.2461	0.2565
RMSE$_l$	0.4748	0.4839	0.4392	0.4378	0.4500
MAE$_l$	0.4036	0.4092	0.3801	0.3580	0.3679

$Q = 16$,ov	$Q = 32$,no	$Q = 32$,ov	$Q = 64$,no	$Q = 64$,ov	$Q = 128$,no
0.2459	0.3516	0.2623	0.3548	0.2735	0.3652
0.1776	0.2614	0.1976	0.2719	0.2134	0.2818
0.3137	0.4494	0.3319	0.4487	0.3421	0.4486
0.2490	0.3693	0.2705	0.3744	0.2871	0.3671

TABLE II

Integral and local MAE and RMSE in filtering of $f_{1,3}(t)$ corrupted with Cauchy noise with $\gamma = 0.1$

	$Q = 1$,no	$Q = 2$,no	$Q = 4$,no	$Q = 8$,no	$Q = 16$,no
RMSE	0.3062	0.3204	0.2740	0.2405	0.2526
MAE	0.1731	0.1914	0.1810	0.1679	0.1725
RMSE$_l$	0.5653	0.5866	0.4793	0.4206	0.4351
MAE$_l$	0.4932	0.5093	0.4078	0.3674	0.3679

$Q = 16$,ov	$Q = 32$,no	$Q = 32$,ov	$Q = 64$,no	$Q = 64$,ov	$Q = 128$,no
0.1857	0.2635	0.2037	0.2730	0.2215	0.2974
0.1306	0.1881	0.1492	0.2041	0.1691	0.2254
0.3127	0.4419	0.3357	0.4385	03530	0.4524
0.2471	0.3571	0.2678	0.3560	0.2868	0.3638

TABLE III

Integral and local MAE and RMSE in filtering of $f_{1,6}(t)$ corrupted with Cauchy noise with $\gamma = 0.1$.

	$Q = 1$,no	$Q = 2$,no	$Q = 4$,no	$Q = 8$,no	$Q = 16$,no
RMSE	0.2116	0.2102	0.2004	0.2020	0.1893
MAE	**0.0996**	0.1056	0.1218	0.1278	0.1445
RMSE$_l$	0.6513	0.6407	0.5845	0.5584	0.4679
MAE$_l$	0.5839	0.5738	0.5135	0.4819	0.4105

$Q = 16$,ov	$Q = 32$,no	$Q = 32$,ov	$Q = 64$,no	$Q = 64$,ov	$Q = 128$,no
0.1461	0.1852	0.1478	0.1990	0.1646	0.2347
0.1151	0.1508	0.1260	0.1698	0.1429	0.1942
0.3674	0.4166	**0.3272**	0.4108	0.3388	0.4377
0.3060	0.3387	**0.2617**	0.3455	0.2724	0.3497

TABLE IV

INTEGRAL AND LOCAL MAE AND RMSE IN FILTERING OF $f_{2,1}(t)$ CORRUPTED WITH CAUCHY NOISE WITH $\gamma = 0.1$.

	$Q = 1$,no	$Q = 2$,no	$Q = 4$,no	$Q = 8$,no	$Q = 16$,no
RMSE	0.3784	0.3969	0.3407	0.3308	0.3545
MAE	0.3016	0.3166	0.2616	0.2517	0.2640
RMSE_l	0.4788	0.4998	0.4384	0.4242	0.4545
MAE_l	0.4130	0.4279	0.3799	0.3628	0.3774
$Q = 16$,ov	$Q = 32$,no	$Q = 32$,ov	$Q = 64$,no	$Q = 64$,ov	$Q = 128$,no
0.2486	0.3891	0.2767	0.4250	0.3185	0.5052
0.1736	0.2809	0.1994	0.3162	0.2420	0.3707
0.3169	0.4980	0.3515	0.5425	0.4152	0.6410
0.2420	0.3978	0.2747	0.4474	0.3347	0.5174

TABLE V

INTEGRAL AND LOCAL MAE AND RMSE IN FILTERING OF $f_{2,3}(t)$ CORRUPTED WITH CAUCHY NOISE WITH $\gamma = 0.1$.

	$Q = 1$,no	$Q = 2$,no	$Q = 4$,no	$Q = 8$,no	$Q = 16$,no
RMSE	0.3011	0.3200	0.2773	0.2410	0.2462
MAE	0.1727	0.1946	0.1841	0.1665	0.1739
RMSE_l	0.5548	0.5837	0.4832	0.4238	0.4231
MAE_l	0.4837	0.5079	0.4130	0.3689	0.3553
$Q = 16$,ov	$Q = 32$,no	$Q = 32$,ov	$Q = 64$,no	$Q = 64$,ov	$Q = 128$,no
0.1728	0.2697	0.1948	0.3051	0.2348	0.2773
0.1235	0.1908	0.1439	0.2204	0.1751	0.1841
0.2882	0.4555	0.3202	0.5104	0.3837	0.6139
0.2283	0.3691	0.2575	0.4196	0.3122	0.4989

TABLE VI

INTEGRAL AND LOCAL MAE AND RMSE IN FILTERING OF $f_{2,6}(t)$ CORRUPTED WITH CAUCHY NOISE WITH $\gamma = 0.1$.

	$Q = 1$,no	$Q = 2$,no	$Q = 4$,no	$Q = 8$,no	$Q = 16$,no
RMSE	0.2079	0.2121	0.2039	0.2011	0.1913
MAE	**0.0897**	0.0970	0.1145	0.1283	0.1356
RMSE_l	0.6389	0.6466	0.5925	0.5528	0.4676
MAE_l	0.5708	0.5756	0.5193	0.4785	0.4040
$Q = 16$,ov	$Q = 32$,no	$Q = 32$,ov	$Q = 64$,no	$Q = 64$,ov	$Q = 128$,no
0.1376	0.1943	0.1464	0.2223	0.1684	0.2645
0.1033	0.1468	0.1172	0.1722	0.1380	0.1983
0.3278	0.4481	**0.3241**	0.5117	0.3679	0.5757
0.2755	0.3769	**0.2585**	0.4230	0.3098	0.4788

TABLE VII

Integral and local MAE and RMSE in filtering of $f_3(t)$ corrupted with Cauchy noise with $\gamma = 0.1$.

	$Q=1$,no	$Q=2$,no	$Q=4$,no	$Q=8$,no	$Q=16$,no
RMSE	0.3535	0.3313	0.3502	0.2993	0.2813
MAE	0.2257	0.2236	0.2470	0.2176	0.2020
RMSE_l	0.5715	0.5287	0.5504	0.4641	0.4348
MAE_l	0.4995	0.4570	0.4638	0.4094	0.3672
$Q=16$,ov	$Q=32$,no	$Q=32$,ov	$Q=64$,no	$Q=64$,ov	$Q=128$,no
0.2050	0.3031	0.2317	0.3305	0.2549	0.3549
0.1450	0.2202	0.1657	0.2366	0.1854	0.2582
0.3115	0.4595	0.3476	0.5018	0.3798	0.5195
0.2467	0.3806	0.2703	0.4067	0.2986	0.4112

nation of optimal parameter κ used in the ICI algorithm in [30], [31] for determination of the multiplicative parameter $\kappa\rho$. This technique will be realized in the following manner. A set of $\Gamma_l \in \mathbf{\Gamma}$ values is considered, where Γ_l represents different possible values of $\kappa\rho$. For each $\Gamma_l \in \mathbf{\Gamma}$, the ICI algorithm is applied to the signal obtained for different widths of intervals $\hat{f}_{\xi_i}(n)$. Let the obtained estimates be denoted by $\hat{f}_{\Gamma_l}(n)$, and adaptive intervals width by $\xi_{\Gamma_l}(n)$, where index denotes the used parameter Γ_l. According to the CV criterion, the optimal value of Γ_l can be determined based on the following minimization problem:

$$\Gamma_{opt} = \arg\min_{\Gamma_l \in \mathbf{\Gamma}} \sum_n \frac{[x(n) - \hat{f}_{\Gamma_l}(n)]^2}{1 - 1/\xi_{\Gamma_l}(n)}. \quad (22)$$

Then, we adopt $\hat{f}_{\Gamma_{opt}}(n)$ as an output of the adaptive filter while $\xi_{\Gamma_{opt}}(n)$ is the optimal width of adaptive intervals.

In addition, we should note that the obtained estimate could have errors in estimation of the adaptive intervals width. Sources of these errors are in probabilistic nature of the ICI rule. These errors are studied in details in [18], [30]. A common technique to solve this problem is a median filtering of adaptive parameter (interval width) and selecting output estimate according to the obtained filtered adaptive interval width.

Note that the main difference between the proposed algorithm and the original ICI algorithm is in the technique used in filtering stage to obtain estimates $\hat{f}_{\xi_i}(n)$. In the ICI algorithm this filtering is performed in the time-domain by using the convolution. This is suitable for signals that are relatively low-pass, but the proposed technique, where filtering is performed in the frequency domain using the robust DFT, is suitable for signals with relatively high frequency content. Note that this opens possibilities to combine the original algorithm for intervals of relatively low frequency content (with possible abrupts in the signal) with the proposed robust DFT-based algorithm applied for signals of high frequency content.

Example. The signal $f_{1,6}(t)$ has been considered with the parameters as in the previous section. It is corrupted with the Cauchy noise $\alpha = 1$ and $\gamma = 0.1$. Signal is filtered with non-overlapped intervals of the width $\xi_i \in \Xi = \{8, 16, 32, 64, 128, 256\}$. The same procedure could be done with the overlapped segments. Fig. 6a represents the original and noisy signal, while Figs. 6b-d show signal filtered with $\xi_6 = 256$, $\xi_4 = 64$ and $\xi_2 = 16$. For the CV algorithm we have considered $\Gamma_l \in \mathbf{\Gamma}$ where $\Gamma_l = 10^{-1+0.1l}$, with $l \in [0, 40]$. The obtained adaptive estimate is given in Fig. 6e, with the corresponding adaptive window width given in Fig. 6g. It can be seen that the obtained intervals are wider in the noise only region, while in the region of signal variations intervals are going to be smaller. However, the adaptive interval width is the subject to considerable errors and we have applied the median filtering of the window size 5 to the adaptive interval widths. The obtained adaptive interval width

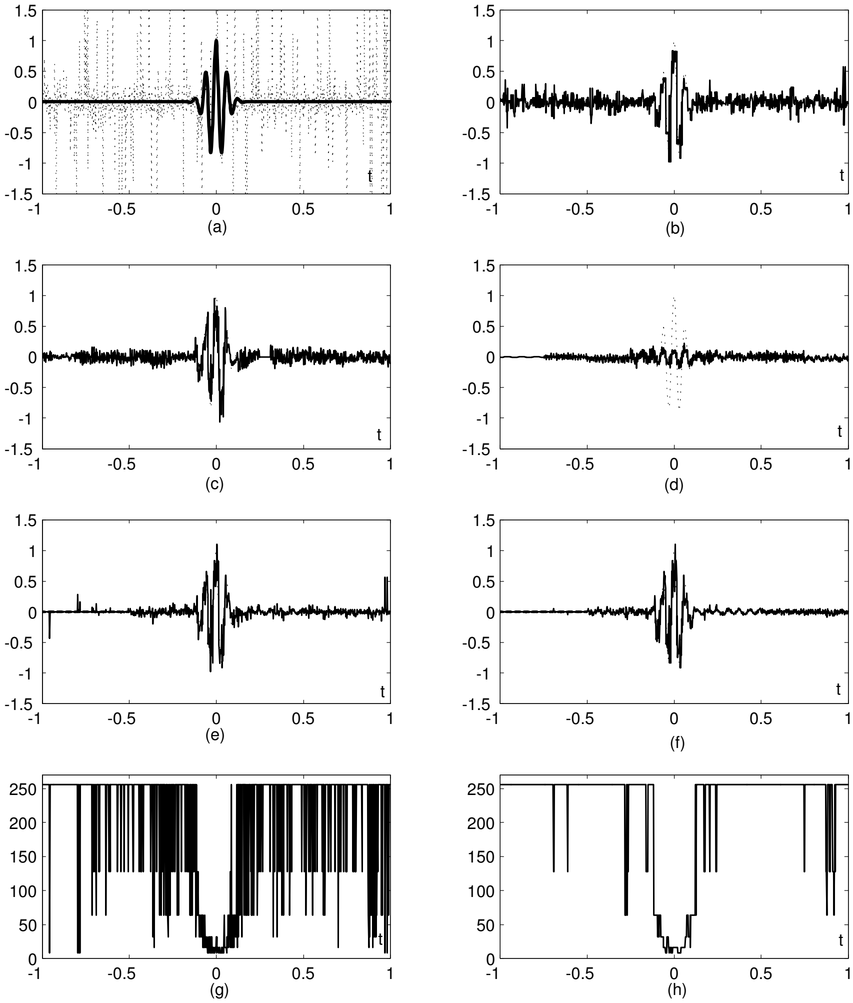

Fig. 6. Adaptive filtering of signal $f_{1,6}(t)$ embedded in the α-stable noise with $\alpha = 1$ (Cauchy noise) with dispersion $\gamma = 0.1$: (a) Original signal - thick line; noisy signal dashed line; (b) The signal filtered with nonoverlapped intervals of constant width $\xi = 8$; (c) The signal filtered with nonoverlapped intervals of constant width $\xi = 32$; (d) The signal filtered with nonoverlapped intervals of constant width $\xi = 256$; (e) The signal filtered with adaptive algorithm; (f) The signal filtered with adaptive algorithm and median filtering applied to the adaptive interval width; (g) Adaptive interval width (given in number of samples); (h) Adaptive interval width filtered with median filter (given in number of samples).

is given in Fig. 6h, and it can be seen that the behavior of this parameter is as expected. The corresponding adaptive estimate is given in Fig. 6f. Here, we can see that the resulting estimate produces accurate results for signal region, and, at the same time, relatively small amount of residual noise remains in the noise only region.

Finally, we considered the Monte Carlo simulation for this signal and for the Cauchy noise but for dispersion factor $\gamma \in [0, 0.3]$. For each considered value γ we repeated the simulations 100 times. The obtained MAE is presented in Fig. 7. It can be seen that the proposed algorithm with applied median filtering outperforms the constant interval length algorithms for relatively wide range of γ values ($\gamma \in [0, 0.25]$) and, more importantly, the

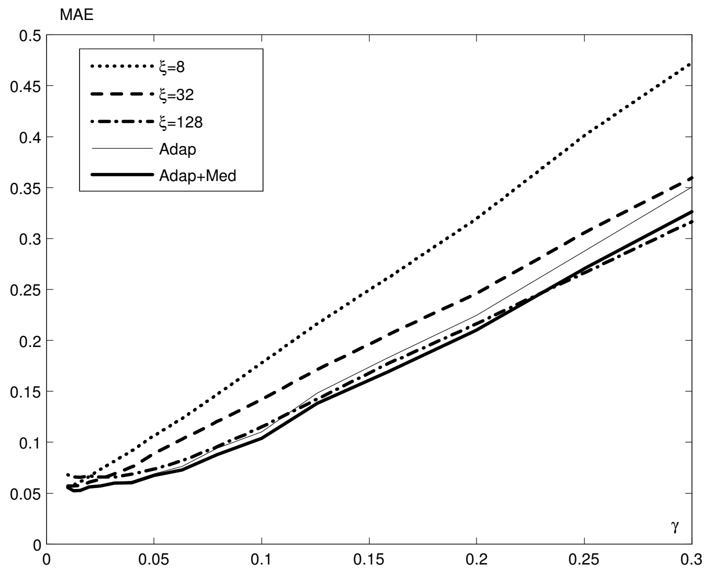

Fig. 7. MAE for signal $f_{1,6}(t)$ embedded in the α-stable noise with $\alpha = 1$ (Cauchy noise) with respect to $\gamma \in [0, 0.3]$ for interval widths $\xi = 8$, $\xi = 32$ and $\xi = 128$ (intervals are non-overlapped) and with applying adaptive algorithm (Adap) and adaptive algorithm with median filtering of the adaptive intervals width (Adap+Med).

proposed algorithm introduces small amplitude distortions in the region of relatively high signal amplitude. For example, for $\gamma = 0.1$ the proposed algorithm produces the MAE of 0.1052, that is better than for all other algorithms considered in Table III, except for the widest intervals case when we have significant distortion of signal with a high magnitude.

VI. Conclusion

The new technique for filtering signals with varying amplitude based on the robust DFT of the signal intervals has been proposed. Both the non-overlapped and overlapped intervals are considered. Use of the latter approach shows significant improvement over the former for all widths of intervals. It has been shown that the proposed improvement of the algorithm is not paid by increasing calculation complexity with respect to the robust DFT calculated over entire interval. The shorter intervals cause increasing of the noise influence. Then, the adaptive algorithm inspired by the ICI rule is proposed to produce a trade-off between noise influence and errors caused by variations in the signal amplitude. This algorithm has shown excellent accuracy and it provides the adaptive interval width.

There are numerous potential further steps in this research, including: analysis of real-valued signals embedded in real-valued noise; applications in radar signal and speech processing; employing optimal or adaptive robust DFT forms; extension toward 2D and multidimensional signals with application in filtering of optical interferograms. Also, we are planning to consider several refinement strategies for the algorithm. These strategies include better selection of the start and end points of the intervals; filtering of adaptive intervals width for each obtained Γ_l from the considered set; etc. In any case, the results for the proposed approach are encouraging and they can be used in several important applications in the presented or in refined form.

References

[1] M. J. Lombardi and S. J. Godsill, "On-line Bayesian estimation of signals in symmetric α-stable noise," *IEEE Trans. Sig. Proc.*, Vol. 54, No. 2, Feb. 2006, pp. 775-779.

[2] D. Radford, A. Kurekin, D. Marshall, K. Lever and V. Lukin: "Robust processing of SAR holo-

gram data to mitigate impulse noise impairments," in *Proc. Fusion*, 2005.

[3] G. R. Arce, *Nonlinear signal processing - a statistical approach*, Wiley 2005.

[4] J. T. Astola and P. Kuosmanen, *Fundamentals of Nonlinear Digital Filtering*, CRC Press, Boca Raton, Fla, USA, 1997.

[5] Z. Wang and D. Zhang, "Progressive switching median filter for the removal of impulse noise from highly corrupted images," *IEEE Trans. Circ. & Syst. II*, Vol. 46, No. 1, pp. 78-80, Jan. 1999.

[6] E. Besdok, "Impulsive noise suppresion from images with a modified two-step iterative median filter," *Jour. of El. Imag.*, Vol. 13, No. 4, pp.714-719, Oct. 2004.

[7] I. Djurović and LJ. Stanković, "Realization of the robust filters in the frequency domain," *IEEE Sig. Proc. Let.*, Vol. 9, No. 10, Oct. 2002, pp.333-335.

[8] G. R. Arce, "A general weighted median filter structure admitting negative weights," *IEEE Trans. Sig. Proc.*, Vol. 46, No. 12, Dec. 1998. pp. 3195-3205.

[9] S. Kalluri and G. R. Arce, "Robust frequency-selective filtering using weighted myriad filters admitting real-valued weights," *IEEE Trans. Sig. Proc.*, Vol. 49, No. 11, Nov. 2001, pp. 2721-2733.

[10] I. Shmulevich and G. R. Arce, "Spectral design of weighted median filters admitting negative weights," *IEEE Sig. Proc. Let.*, Vol. 8, No. 12, pp. 313-316.

[11] G. R. Arce and J. L. Paredes, "Recursive weighted median filters admitting negative weights and their optimization," *IEEE Trans. Sig. Proc.*, Vol. 48, No. 3, Mar. 2000, pp. 768-779.

[12] V. Katkovnik, "Robust M-periodogram," *IEEE Trans. Sig. Proc.*, Vol. 46, No. 11, Nov. 1998, pp. 3104-3109.

[13] V. Katkovnik, "Robust M-estimates of the frequency and amplitude of a complex-valued harmonic," *Signal Processing*, Vol. 77, No. 1, Aug. 1999, pp. 71-84.

[14] P. J. Huber, "Robust regression: asymptotics, conjectures and Monte Carlo," *Ann. math. statistic*, Vol. 1, No. 5, pp. 799-821, 1973.

[15] P. J. Huber, *Robust statistics*, John Wiley & Sons, 1981.

[16] H. A. David and H. N. Nagaraja, *Order statistics*, Wiley, 2003.

[17] V. Katkovnik and LJ. Stanković, "The instantaneous frequency estimation using the Wigner distribution with varying and data-driven window length," *IEEE Trans. Sig. Processing*, Vol. 46, No. 9, Sept. 1998, pp. 2315-2326.

[18] LJ. Stanković and V. Katkovnik, "Algorithm for the instantaneous frequency estimation using time-frequency distributions with variable window width," *IEEE Sig. Proc. Let.*, Vol. 5, No. 9, Sep. 1998, pp. 224-227.

[19] LJ. Stanković and V. Katkovnik. "Instantaneous frequency estimation using higher order distributions with adaptive order and window length", *IEEE Trans. Inf. Th.*, Vol. 46, No. 1, Jan. 2000, pp. 302-311.

[20] I. Djurović, LJ. Stanković and J. F. Böhme, "Myriad filter based form of the DFT," *EUSIPCO'2002*, Toulouse, France, Vol.III, pp. 433-436.

[21] I. Djurović, V. Katkovnik and LJ. Stanković, "Median filter based realizations of the robust time-frequency distributions", *Signal Processing*, Vol.81, No.7, 2001, pp. 1771-1776.

[22] I. Djurović, LJ. Stanković and J. F. Böhme, "Robust L-estimation based forms of signal transforms and time-frequency representations," *IEEE Trans. Sig. Proc.*, Vol. 51, No. 7, July 2003, pp.1753-1761.

[23] I. Djurović, V. V. Lukin and A. A. Roenko, "Removal of α-stable noise in frequency modulated signals using robust DFT forms," *Telecommunications and Radioengineering*, Vol. 61, No. 7, 2004, pp. 574-590.

[24] P. Stoica and R. L. Moses, *Introduction to spectral analysis*, Prentice-Hall, 1997.

[25] P. Welch, "The use of fast Fourier transform for the estimation of power spectra: a method based on time-averaging over short, modified periodograms," *IEEE Trans. on Aud. and Electroacustics*, Vol. 15, No. 2, 1967.

[26] R. Oktem, "Transform domain algorithms for image compression and denoising", PhD Thesis, Tampere University of Technology (Tampere, Finland), 142 p., 2000, http://www.cs.tut.fi/~karen/project_site.

[27] C. L. Nikias and M. Shao, *Signal processing with alpha stable distributions and applications*, New York: Wiley 1995.

[28] G. A. Tsihrintzis and C. L. Nikias, "Performance of optimum and suboptimum receivers in the presence of impulsive noise modeled as an alpha-stable process," *IEEE Trans. Commun.*, Vol. 43, Nos 2-4, Feb-Apr. 2005, pp. 904-914.

[29] A. Goldenshluger and A. Nemirovski, "On spatial adaptive estimation of nonparametric regression", *Math. Meth. Statistics*, Vol .6, 1997, pp. 135-170.

[30] V. Katkovnik, K. Egiazarian and J. Astola, "Adaptive varying window methods in image processing Part I: Denoising and deblurring," TICSP Series Report #13, March 2003.

[31] J. Fan and I. Gijbels, *Local polynomial modeling and its applications*, Chapman & Hall, 1996.